

RESEARCH LETTER

Cell-Autonomous Role
of EGFR in Spontaneous
Duodenal Tumors in LRIG1
Null Mice

Leucine-rich repeats and immunoglobulin-like domains 1 (LRIG1) is a tumor suppressor that negatively regulates the ERBB family, including epidermal growth factor receptor (EGFR), and other receptor tyrosine kinases (RTKs).^{1,2} *Lrig1*^{CreERT2/CreERT2} (functionally *Lrig1* null; hereafter *Lrig1*^{Cre}) mice spontaneously develop duodenal tumors with increased EGFR and ERBB2-3 expression and increased ERK1/2 activity by immunoblotting.³ These *Lrig1* null tumors arise over expanded Brunner glands that exhibit increased expression of the EGFR ligands amphiregulin and betacellulin.⁴ Although EGFR seems to play an important role, these results do not preclude LRIG1 from mediating its effects through other RTKs.

To directly implicate EGFR as the target of LRIG1 in these tumors, we generated *Lrig1*^{Cre/Cre}; *Egfr*^{flox/flox}; *R26R*^{YFP} mice in which knockout of *Egfr* is induced by tamoxifen (TAM) administration in *Lrig1*-expressing cells that are genetically *Lrig1* null. Three daily injections of 2 mg of TAM or corn oil (control) were given to mice at 2 months of age and mice were sacrificed 4 months later. Notably, there were no detectable tumors in half of the TAM-treated mice (8/16), and the tumors that did form were smaller than those in control mice (Figure 1A). Tumors in both groups exhibited low-grade dysplasia overlying expanded Brunner glands and an ill-defined boundary between the tumor epithelium and Brunner glands,⁴ along with mild lymphoplasmacytic infiltration and lamina propria expansion. Tumors were histopathologically indistinguishable (Figure 1B and Supplementary Figure 1A and B). We confirmed efficient recombination as determined by YFP expression (Supplementary Figure 1C).

Although recent work has identified a role for EGFR in the stroma for intestinal and hepatic neoplasia,^{5,6} we elected to examine EGFR and

LRIG1 expression in mouse duodenal epithelium. To that end, we used *Egfr*^{Emerald GFP} (*Egfr*^{Em})⁷ and *Lrig1*^{Apple} (*Lrig1*^{Ap})⁸ reporter mice that track EGFR protein and *Lrig1* transcriptional activity, respectively. As expected, duodenal tumors developed in *Lrig1* null (*Lrig1*^{Ap/Ap}; *Egfr*^{Em/+}) mice, but not in *Lrig1* heterozygous (*Lrig1*^{Ap/+}; *Egfr*^{Em/+}) mice. In *Lrig1*^{Ap/Ap}; *Egfr*^{Em/+} mice, *Egfr*^{Em} staining was detected in the tumor and stroma (Figure 1C and Supplementary Figure 2). However, *Lrig1*^{Ap} fluorescence was restricted to the tumor epithelium (Figure 1C). In addition, *Lrig1*^{Cre}-driven recombination was observed only in the epithelium (Supplementary Figure 1C). Although we do not dispute the impact of stromal EGFR on intestinal neoplasia, these results establish that LRIG1 has an epithelial, cell-autonomous, EGFR-dependent tumor suppressor activity for spontaneously forming mouse duodenal tumors.

We next sought to determine the mechanism of tumor formation in the absence of EGFR in *Lrig1* null mice. Given the importance of canonical Wnt signaling in gastrointestinal neoplasia, we examined β -catenin immunofluorescence because cytoplasmic and nuclear β -catenin immunoreactivity is a hallmark of Wnt pathway activation. As previously described,³ administration of TAM to *Lrig1*^{Cre/+}; *Apc*^{flox/+} mice results in elimination of 1 *Apc* allele with tumors appearing 50 days later throughout the gastrointestinal tract because of stochastic loss of the second *Apc* allele. Duodenal tumors from these mice showed cytoplasmic and nuclear β -catenin staining throughout the tumor, whereas β -catenin was membranous in normal epithelium (Figure 1D). In marked contrast, β -catenin retained a plasma membrane-dominant staining in *Lrig1* null spontaneous duodenal tumors in the presence or absence of EGFR (Figure 1D). Because *Lrig1* negatively regulates other ERBBs and RTKs, we probed a commercial mouse RTK array using tissue lysates from *Lrig1*^{Cre/Cre}; *Egfr*^{flox/flox}; *R26R*^{YFP} tumors. In the tumors from oil-treated mice, ERBB2 had the highest activity of the ERBBs followed by EGFR and ERBB3, whereas there was no detectable ERBB4

activity; modest PDGFRA and RON activity was observed (Figure 2A and Supplementary Figure 3). In TAM-treated mice, there was an expected absence of EGFR activity. ERBB3 activity increased 1.5-fold and was the only RTK to show increased activity on loss of EGFR (Figure 2A and B and Supplementary Figure 3). Of note, ERBB3 immunoreactivity was restricted to the tumor epithelium in the presence or absence of EGFR (Figure 2C). Finally, we considered what endogenous ligand might be activating ERBB3 and ERBB3/ERBB2 heterodimers; ERBB2 has no known ligand but is the preferred heterodimer for the other ERBBs. Among the ERBB3/4 ligands, only neuregulin 1 (*Nrg1*) was increased in duodenal tumors compared with adjacent normal tissue (Figure 2D and Supplementary Figure 4A). We observed NRG1 staining in the stroma of *Lrig1* null duodenal tumors in the presence and absence of EGFR, suggesting it may be the ligand driving ERBB3 and ERBB2 activity (Figure 2E and Supplementary Figure 4B). Taken together, these findings support an epithelial, cell-autonomous role for EGFR in the development of spontaneous duodenal tumors in *Lrig1* null mice. In the absence of EGFR, enhanced ERBB3 activity may be fueled by increased expression of NRG1 in the stroma.

H. NIITSU^{1,a}

Y. LU^{2,a}

W. J. HUH³

A. M. LOVE¹

J. L. FRANKLIN^{1,4}

R. J. COFFEY^{1,4}

¹Department of Medicine, Vanderbilt University Medical Center, Nashville, Tennessee

²Xijing Hospital of Digestive Diseases, Fourth Military Medical University, Xi'an, China

³Department of Pathology, Microbiology, and Immunology, Vanderbilt University Medical Center, Nashville, Tennessee; and ⁴Department of Cell and Developmental Biology, Vanderbilt University, Nashville, Tennessee

Address correspondence to: Robert J. Coffey, MD, Epithelial Biology Center, Vanderbilt University Medical Center, 10415-F MRB IV, 2213 Garland Avenue, Nashville, Tennessee 37232. e-mail: meghan.oloughlin@vmc.org; fax: (615) 343-1591.

References

1. Wang Y, et al. *Br J Cancer* 2013; 108:1765-1770.
2. Simion C, et al. *Endocr Relat Cancer* 2014;21:R431-443.

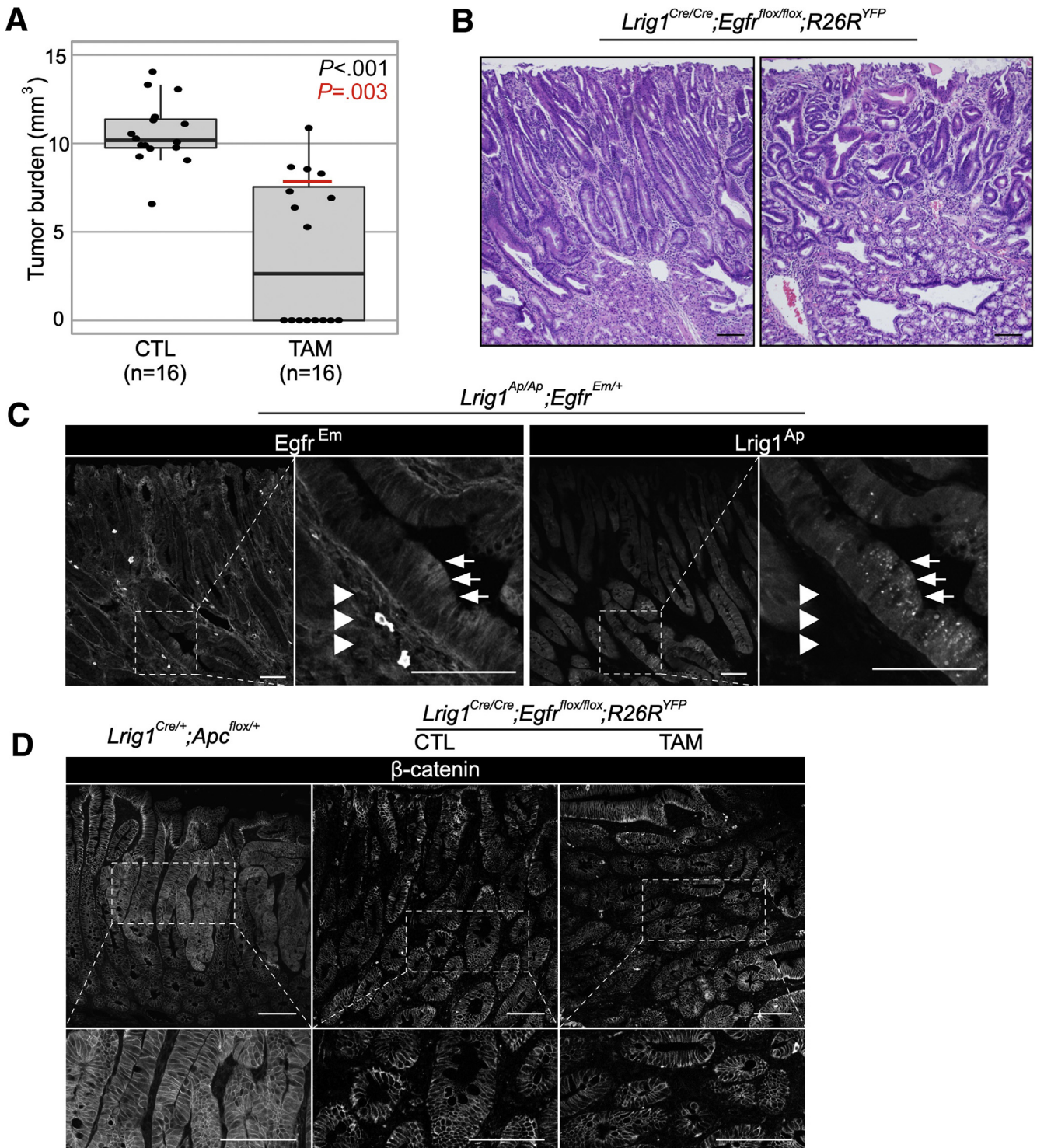


Figure 1. Effect of conditional knockout of *Egfr* on duodenal tumor burden in *Lrig1* null mice. (A) Comparison of tumor burden of duodenal tumors from $Lrig1^{Cre/Cre};Egfr^{flox/flox};R26R^{YFP}$ mice treated with TAM or corn oil (CTL). Red line over the box-plot of TAM group indicates median value when mice without tumors were excluded. (B) Histology of duodenal tumors that develop in the TAM and CTL groups. (C) Greyscale $Egfr^{Em}$ fluorescence (anti-GFP staining) and $Lrig1^{Ap}$ fluorescence in spontaneous duodenal tumors from $Lrig1^{Ap/Ap};Egfr^{Em/+}$ mice. Arrows and arrowheads indicate $Egfr^{Em}/Lrig1^{Ap}$ -positive tumor cells and $Egfr^{Em}$ -positive and $Lrig1^{Ap}$ -negative stroma, respectively. (D) Greyscale immunofluorescence for β -catenin. Left: duodenal tumor from $Lrig1^{Cre/+};Apc^{flox/+}$ mouse. Center and right: duodenal tumor from $Lrig1^{Cre/Cre};Egfr^{flox/flox};R26R^{YFP}$ treated with corn oil (center) and TAM (right), respectively. Scale bar = 100 μm . CTL, control.

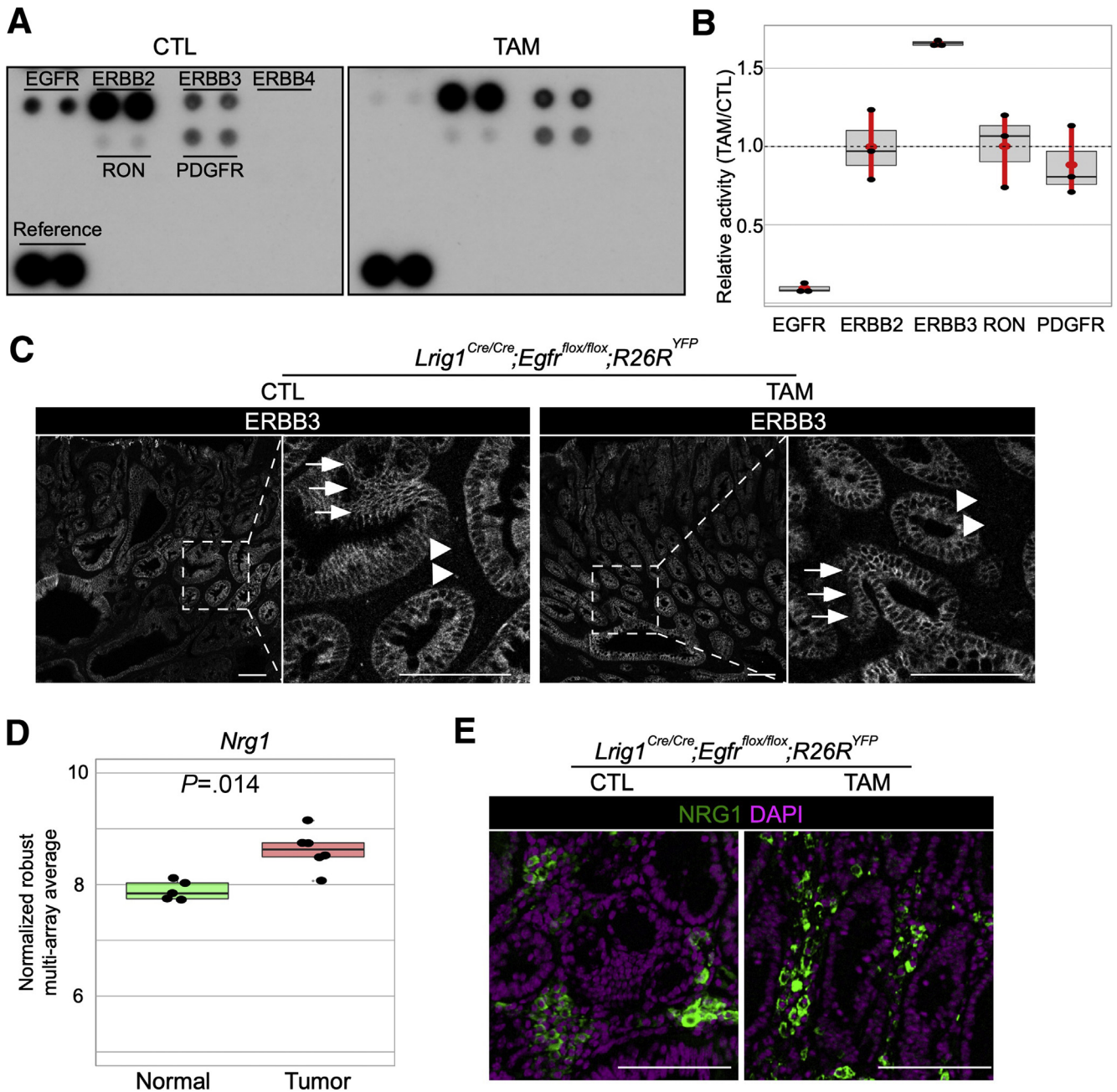



Figure 2. ERBB3 activity is increased in the absence of EGFR in *Lrig1* null duodenal tumors. (A) Representative blots from 3 independent mouse RTK arrays (R&D Systems, Minneapolis, MN). (B) Relative activity of ERBB2, ERBB3, RON, and PDGFRA in TAM-treated group compared with CTL, calculated from RTK array. Red bars indicate 95% confidence intervals. (C) Greyscale immunofluorescence for ERBB3 in TAM-treated and CTL mice. Arrows and arrowheads indicate tumor cells and stroma, respectively. (D) Comparison of *Nrg1* expression by microarray analysis between duodenal tumors and adjacent normal duodenum in *Lrig1* null mice. (E) Immunofluorescence for NRG1 (green) with DAPI (purple) in duodenal tumors from CTL and TAM-treated mice. Scale bar = 100 μ m.

3. Powell AE, et al. Cell 2012; 149:146–158.
4. Wang Y, et al. Am J Pathol 2015; 185:1123–1134.
5. Hardbower DM, et al. Oncogene 2017;36:3807–3819.
6. Srivatsa S, et al. Gastroenterology 2017;153:178–190.
7. Yang YP, et al. Cell Rep 2017; 19:1257–1267.
8. Poulin EJ, et al. Stem Cell Res 2014;13:422–430.

^aAuthors share co-first authorship.

 Most current article

© 2021 The Authors. Published by Elsevier Inc. on behalf of the AGA Institute. This is an open access article under the CC BY-NC-ND license (<http://creativecommons.org/licenses/by-nc-nd/4.0/>).
2352-345X
<https://doi.org/10.1016/j.jcmgh.2021.05.004>

Received March 29, 2021. Accepted May 4, 2021.

Conflicts of interest

The authors disclose no conflicts.

Funding

This work was supported by National Cancer Institute R35CA197570 and GI Special Programs of Research Excellence P50CA236733 (to R.J.C.) and Japan Society for the Promotion of Science Oversea Research Fellowship (to H.N.). The authors thank Sarah E. Glass for editorial assistance and acknowledge the generous support of the Nicholas Tierney GI Cancer Memorial Fund.

Supplementary Methods

Mice

Lrig1^{Cre}, *Lrig1^{AP}*, and *Egfr^{Em}* mice were generated as described previously.^{1–3} *Apc^{fllox}* and *R26R^{YFP}* mice were obtained from Jackson Laboratory (Bar Harbor, ME), and *Egfr^{fllox}* mice were generously provided by David Threadgill.⁴ All injections were performed intraperitoneally, including tamoxifen (TAM; Sigma, St. Louis, MO). TAM was dissolved in corn oil and corn oil served as vehicle control. Tissues were harvested immediately after euthanizing mice with carbon dioxide and subsequent cervical dislocation. Duodenal tumor burden was calculated by ex vivo analysis of tumors by magnetic resonance imaging (MRI).

Tissue Preparation for Staining, Histologic Analysis, and Immunofluorescence

Specimens were harvested, immediately fixed with 4% paraformaldehyde in phosphate-buffered saline for 4 hours at 4°C, and then processed as paraffin blocks. Five-micrometer sections were prepared for tissue staining. H&E staining was performed for histologic analysis. Heat-induced epitope retrieval

methods were used to prepare paraffin sections for immunofluorescence in acid citrate buffer (pH 6). All sections for immunofluorescence were blocked with 5% normal donkey serum and 3% bovine serum albumin at 22°C for 1 hour. The primary antibodies used were: anti-GFP (Abcam, #ab5450, 1:500); anti- β -catenin (clone 12F7D1, Vanderbilt Antibody and Protein Resource, 1:200); anti-ERBB3 (Cell Signaling, #12708, 1:100); and anti-NGR1 (Abcam, #ab53104), followed by the appropriated fluorophore-conjugated secondary antibodies. All micrographs were collected with a Nikon A1R laser confocal microscope.

Mouse RTK Array

Proteome Profiler Mouse Phospho-RTK Array Kit (#ARY014, R&D Systems, Minneapolis, MN) was used in accordance with the manufacturer's protocol. In brief, samples were minced and sonicated at 4°C using provided lysis buffer with protease inhibitors (aprotinin, leupeptin, and pepstatin at 10 μ g/mL final concentration), and centrifuged at 14,000 rpm for 5 minutes to collect the supernatant for analysis. After blocking arrays with the provided buffer, samples

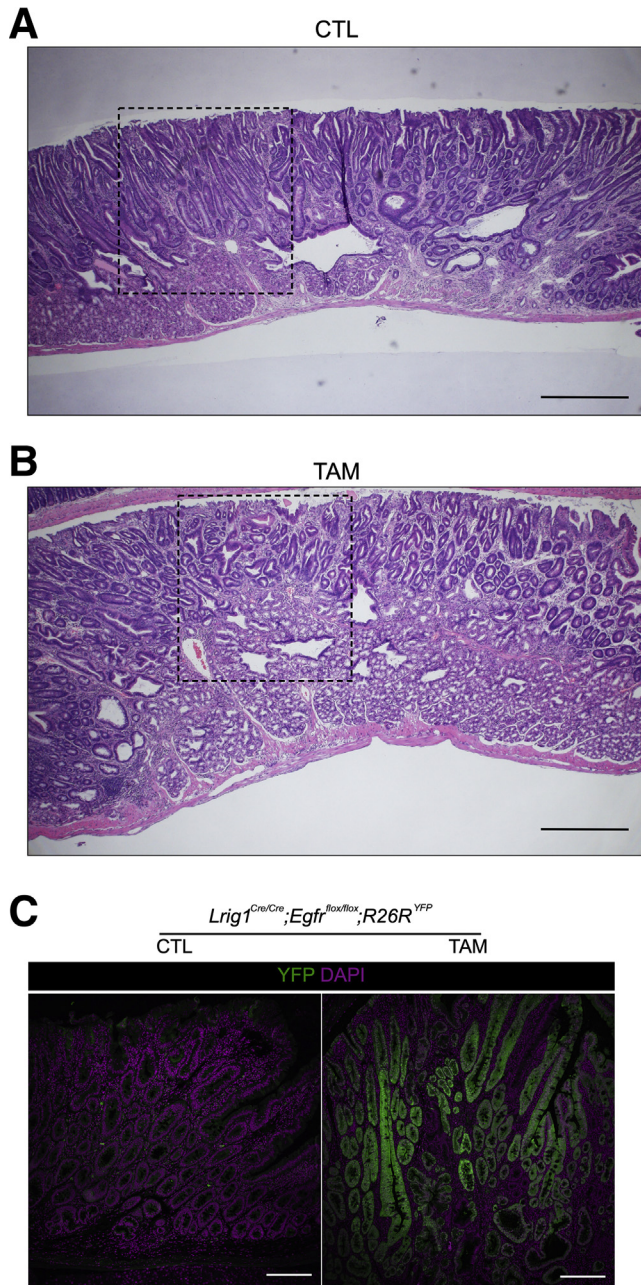
containing 200 μ g of protein were applied to the arrays and incubated at 4°C overnight on a rocking platform. Arrays were labeled with anti-phospho-tyrosine-HRP detection antibody, developed using chemiluminescence, and detected using film.

Statistical Analysis

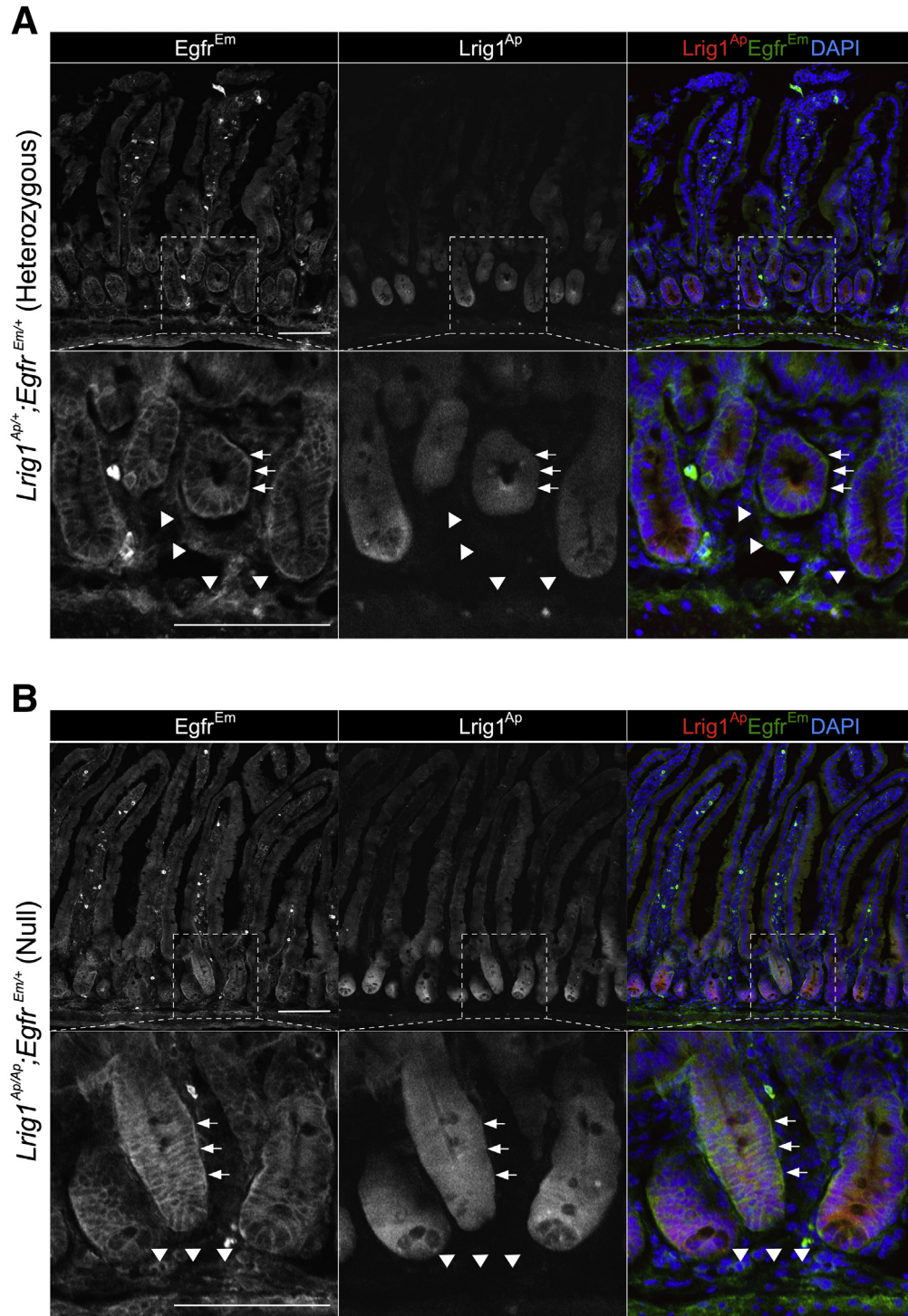
All experiments were repeated at least 3 times. The values are presented in box plots overlaying dot plots; the 95% confidence intervals with median are shown in Figure 2B. For statistical analysis, Wilcoxon rank sum tests were performed and $P < .05$ was considered significant. Statistical analyses were performed using R statistical software version R3.4.3 (R Foundation for Statistical Computing, Vienna, Austria).

Supplementary References

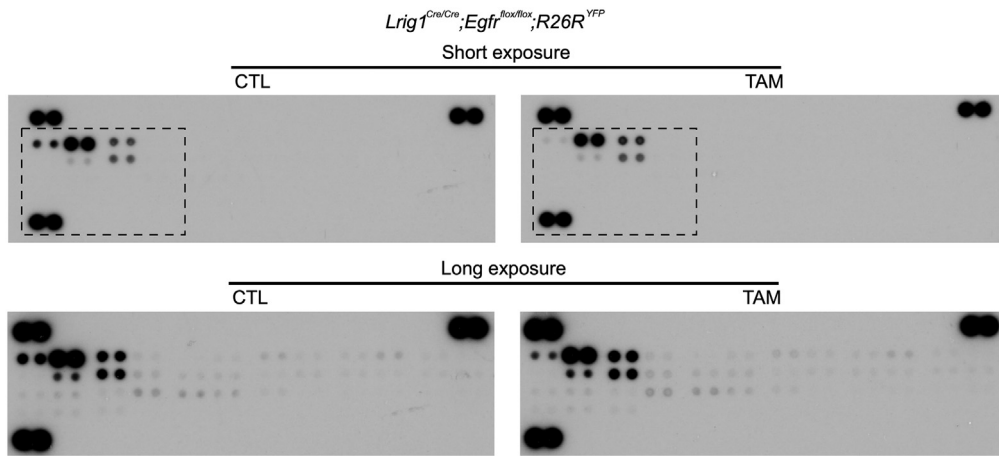
1. Powell AE, et al. *Cell* 2012; 149:146–158.
2. Poulin EJ, et al. *Stem Cell Res* 2014;13:422–430.
3. Yang YP, et al. *Cell Rep* 2017; 19:1257–1267.
4. Lee TC, et al. *Genesis* 2009; 47:85–92.



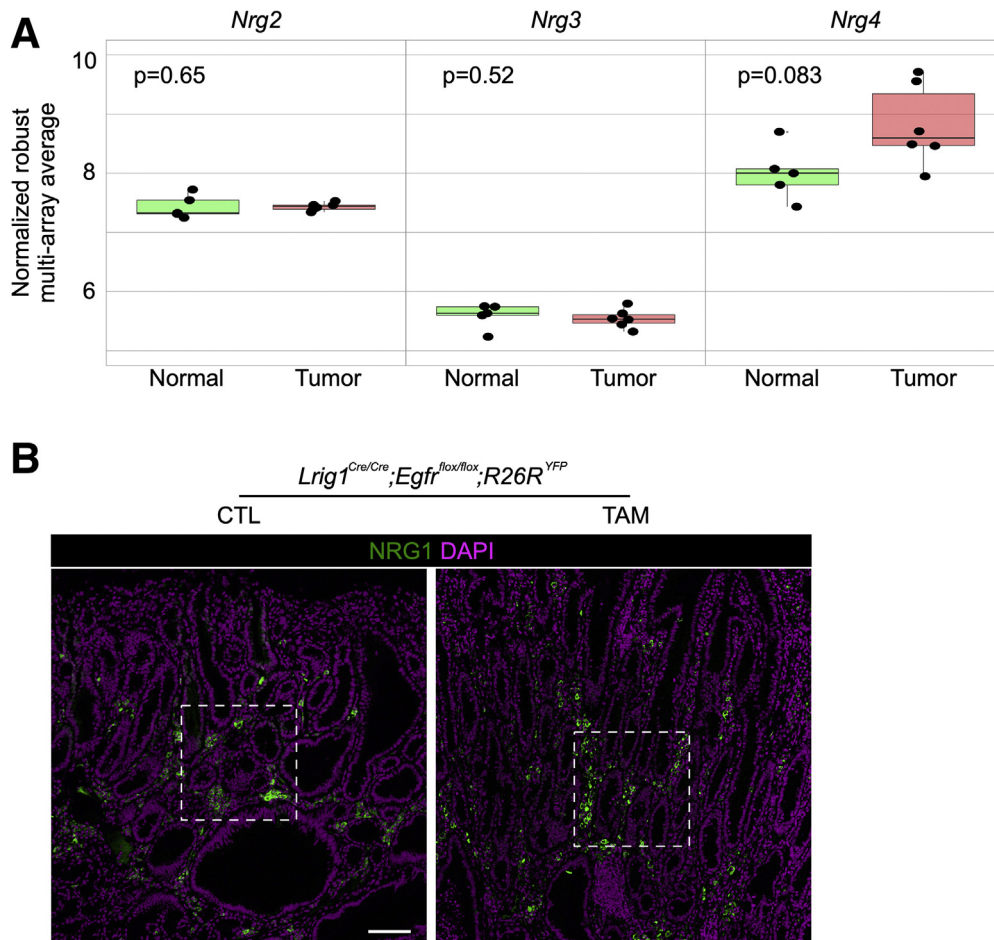
Supplementary Figure 1. Spontaneous duodenal tumors in the presence or absence of EGFR in *Lrig1* null mice. H&E staining for spontaneous duodenal tumors in $Lrig1^{Cre/Cre};Egfr^{flx/flx};R26R^{YFP}$ treated with corn oil (A) or TAM (B). Black lines correspond to enlarged micrographs in Figure 1B. Scale bar = 500 μ m. (C) Immunofluorescence for YFP (green, anti-GFP staining) with DAPI (purple). YFP expression indicates the cells in which $Lrig1^{Cre}$ -driven recombination occurs. Scale bar = 100 μ m. CTL, control.



Supplementary Figure 2. EGFR localization in normal duodenum in $Lrig1^{Ap/+};Egfr^{Em/+}$ and $Lrig1^{Ap/AP};Egfr^{Em/+}$ mice. Immunofluorescence for $Egfr^{Em}$ (green, anti-GFP staining) and $Lrig1^{Ap}$ (red, endogenous fluorescence) in normal duodenum from $Lrig1^{Ap/+};Egfr^{Em/+}$ (A) and $Lrig1^{Ap/AP};Egfr^{Em/+}$ (B) mice. Arrows and arrowheads indicate $Egfr^{Em}/Lrig1^{Ap}$ -positive cells, and $Egfr^{Em}$ -positive and $Lrig1^{Ap}$ -negative stroma, respectively. Scale bar = 100 μ m.



Supplementary Figure 3. Mouse RTK array to compare RTK activity in *Lrig1* null duodenal tumors in the presence and absence of EGFR. Representative blots of RTK array in CTL and TAM groups with short and long exposure. *Black lines* delineate short exposure blots and correspond to enlarged blot shown in [Figure 2A](#).



Supplementary Figure 4. Expression of ERBB3/4 ligands in *Lrig1* null duodenal tumors compared to adjacent normal duodenum. (A) Comparison of *Nrg2-4* expression by microarray analysis between duodenal tumors and adjacent normal duodenum in *Lrig1* null mice. (B) Immunofluorescence for NRG1 (green) with DAPI (purple) in duodenal tumors from CTL and TAM groups. *White lines* delineate are those corresponding to [Figure 2E](#).